



# Integrative metabolomics and gut microbiota analyses reveal the protective effects of DHA-enriched phosphatidylserine on bisphenol A-induced intestinal damage

Qiaoling Zhao<sup>a,1</sup>, Fei Yang<sup>b,1</sup>, Qiuyan Pu<sup>c,1</sup>, Rui Zhao<sup>c</sup>, Su Jiang<sup>d</sup>, Yunping Tang<sup>c,\*</sup>

<sup>a</sup> Zhoushan Institute for Food and Drug Control, Zhoushan, 316000, China

<sup>b</sup> Hangzhou Women's Hospital (Hangzhou Maternity and Child Health Care Hospital), Neonatal Intensive Care Unit, Hangzhou, 310008, China

<sup>c</sup> School of Food and Pharmacy, Zhejiang Ocean University, Zhoushan 316022, China

<sup>d</sup> ECA Healthcare Inc, Shanghai 201101, China

## ARTICLE INFO

### Keywords:

DHA-enriched phosphatidylserine  
Bisphenol A  
Intestinal injury  
Non-targeted metabolomics  
Gut microbiota

## ABSTRACT

The protective effects of docosahexaenoic acid-enriched phosphatidylserine (DHA-PS, 50 or 100 mg/kg) on bisphenol A (BPA)-induced intestinal damage were assessed. The biochemical indices, pathological examination, non-targeted metabolomics integrated with gut microbiota analysis, and immunofluorescence analysis were used to investigate the protective effects of DHA-PS and its underlying regulatory mechanism. The DHA-PS treatment improved the pathology of intestinal tract and increased the expression levels of Claudin-1, Occludin, and ZO-1. In addition, the DHA-PS treatment also notably decreased the levels of interleukin (IL)-1 $\beta$ , IL-6, and tumor necrosis factor (TNF)- $\alpha$ , and increased the antioxidant enzymes activities. Moreover, DHA-PS treatment increased the relative abundances of *Akkermansia*, *Alistipes*, *Butyrivibrio*, *Coriobacteriaceae*\_UCG-002, *Enterorhabdus*, and *Lachnospiraceae*\_UCG-006. DHA-PS treatment alleviated BPA-induced intestinal damage by regulating the kynurenine pathway of tryptophan, lipid, and arachidonic acid metabolisms. Overall, this study suggested that DHA-PS could alleviate BPA-induced intestinal damage by enhancing the intestinal barrier integrity, improving gut microbial composition and metabolites, and inhibiting the TLR4/NF- $\kappa$ B pathways.

## 1. Introduction

The health of the intestine, the organ with the largest contact area in the body, is very important to human health (Camilleri et al., 2012; Garrett et al., 2010). However, the intestinal tract can be affected by different exogenous factors (bacteria, endotoxins, viruses, etc.), which can cause intestinal mucosal damage, intestinal barrier dysfunction, imbalance of internal environmental homeostasis, and enteritis (Groschwitz & Hogan, 2009; Sartor, 2008). Bisphenol A (BPA) is a common industrial substance, which is mainly involved in synthesizing polycarbonate plastic, epoxy resin, and other polymeric materials (Almeida et al., 2018; Ma et al., 2019). Owing to its ubiquitous use, humans are easily exposed to BPA through oral, inhalation, or dermal absorption (Almeida et al., 2018; Song et al., 2019). Increasing studies have demonstrated that long-term exposure to BPA can also cause intestinal dysfunction as well as dysbiosis of gut microbiota (Feng et al.,

2020; Wang et al., 2021; Yao et al., 2023a). Therefore, a substantial concern has been raised about the harmful effects of BPA on intestinal health, and the strategies to alleviate its damaging effects are explored.

Marine phospholipids (PLs), especially docosahexaenoic acid (DHA)- and eicosapentaenoic acid (EPA)-enriched PLs, have multiple beneficial effects on human health, including protecting liver and kidney, improving memory, relieving inflammatory responses, and regulating the composition of gut microbiota (Li et al., 2022; Liu et al., 2017; Qian et al., 2022; Tang et al., 2023; Zhang et al., 2019). Recent studies have demonstrated that marine PL treatment can improve the intestinal barrier. For example, Cao et al. (Cao et al., 2019) revealed that DHA-PL and EPA-PL could effectively ameliorate chronic stress-caused murine intestinal dysfunction. Che et al. (Che et al., 2021) revealed that DHA-PL showed outstanding advantages by regulating dextran sodium sulfate-induced inflammatory responses, oxidative stress, and intestinal dysfunction. Du et al. (Du et al., 2022) demonstrated that DHA-PL and

\* Corresponding author.

E-mail address: [tangyunping1985@zjou.edu.cn](mailto:tangyunping1985@zjou.edu.cn) (Y. Tang).

<sup>1</sup> These authors contributed equally to this work and shared first authorship.

EPA-PL could ameliorate lipopolysaccharide (LPS)-induced intestinal dysfunction by activating the SIRT-1/Nrf2 pathway and restraining the NF- $\kappa$ B and MAPK pathways. DHA-enriched phosphatidylserine (DHA-PS) is a unique glycerophospholipid that incorporates the polyunsaturated fatty acid (DHA) at the *sn*-2 position within its molecular structure (Zhang et al., 2019; Zhang et al., 2022). DHA-PS is known for its wide range of biological functions, such as improving cognition, protecting liver and kidney injury, and regulating intestinal flora (Zhang et al., 2019; Zhou et al., 2021). Our previous study revealed that DHA-enriched phosphatidylserine (DHA-PS) could improve the BPA-induced murine nephrotoxicity (Pu et al., 2023). However, whether DHA-PS can improve BPA-induced intestinal damage is still unknown.

The current study investigated the alleviation effects of orally administrated DHA-PS on BPA-induced intestinal damage. For this purpose, different indicators, including the levels of LPS, inflammatory factors, oxidative stress, and tight junction proteins, were analyzed. Additionally, a non-targeted gut metabolomics approach in combination with gut microbiota and immunofluorescence analysis was further used to understand the underlying regulatory mechanism of protecting effects of DHA-PS on BPA-induced intestinal damage. These findings might provide a possible defense against the harmful effects of BPA.

## 2. Materials and methods

### 2.1. Materials and reagents

The BPA (purity > 99%) was supplied by Aladdin (Shanghai, China).

The DHA-PS was prepared as described in our previous studies (Zhang et al., 2023; Zhou et al., 2021). The primary antibodies against NF- $\kappa$ B p65 (AF0246), p-NF- $\kappa$ B p65 (AF5875), and TLR4 (AF8187) were provided by Beyotime (Shanghai, China), while the primary antibodies against Claudin-1 (28674-1-AP), Occludin (13409-1-AP), ZO-1 (21773-1-AP), I $\kappa$ B $\alpha$  (66418-1-Ig), and p-I $\kappa$ B $\alpha$  (82349-1-RR) were provided by Proteintech Group (Wuhan, China).

### 2.2. Animal treatments

After 7 days of acclimatization, male C57BL/6J mice ( $n = 24$ , 5-week-old, weighing 15–17 g) were randomly assigned to 4 groups (Fig. 1A,  $n = 6$  per group), including control group (CON, Milli-Q water), model group (MOD, 5 mg/kg BPA), 50 DHA-PS group (50 mg/kg DHA-PS + 5 mg/kg BPA), and 100 DHA-PS group (100 mg/kg DHA-PS + 5 mg/kg BPA). The mice were all given the normal chow diet and intragastrically administered with BPA (MOD and DHA-PS groups) or a certain amount of Milli-Q water (CON) for 6 weeks. DHA-PS was intragastrically administered half an hour after BPA. Finally, the mice were deprived of water for 12 h and then euthanized by cervical dislocation. Their blood samples were obtained by *retro*-orbital bleeding, and jejunum tissues were removed and preserved for subsequent experiments. The fecal samples were obtained a day before sacrificing animals for the gut microbiota analysis.

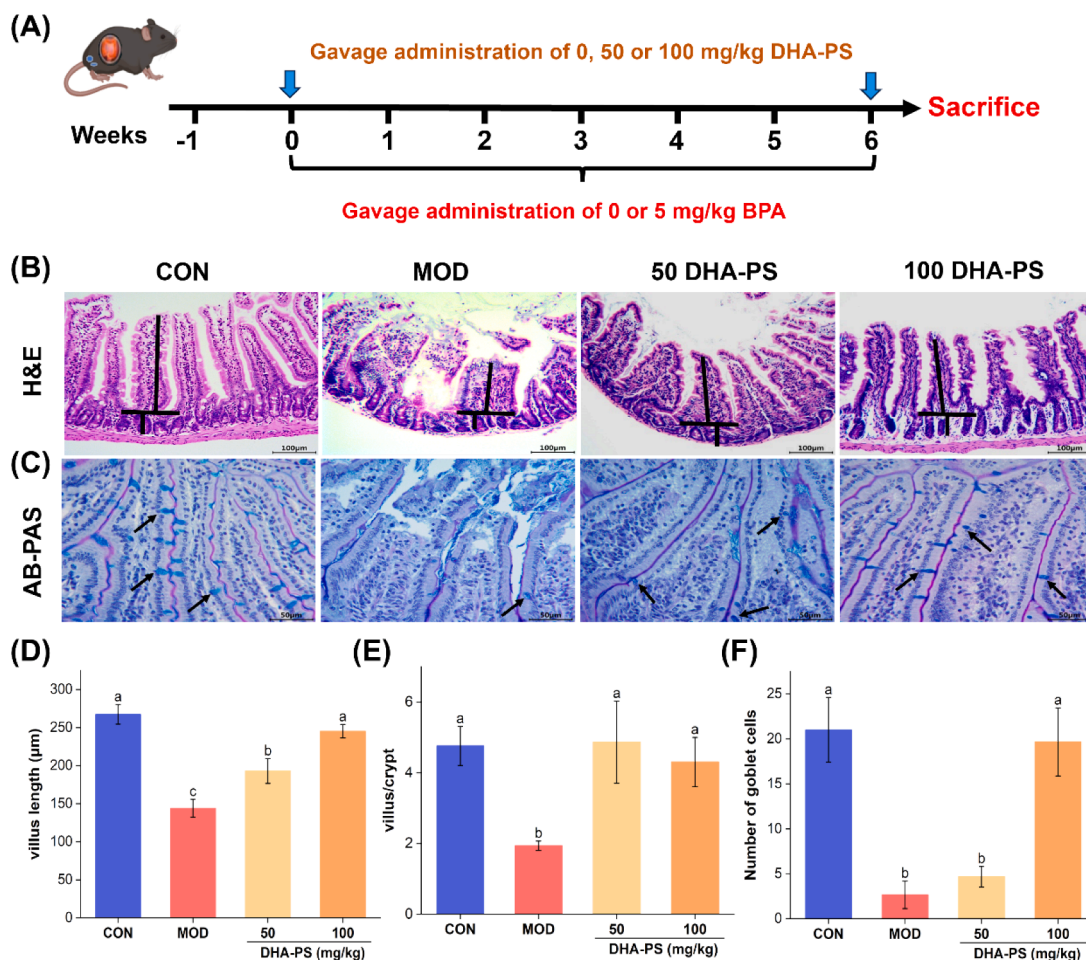


**Fig. 1.** Effects of BPA exposure on the murine jejunum injury. (A) Experimental design ( $n = 6$ ); (B) H&E staining ( $n = 3$ , 400 $\times$ ); (C) AB-PAS staining ( $n = 3$ , 400 $\times$ ), Arrow: the goblet cells; (D) The villus length; (E) The ratio of villus to crypt. Ratio of villi length to crypt depth in the jejunum; (F) The number of goblet cells per 4 villi. Different letters over bars indicate statistical significance between two groups ( $P < 0.05$ ), the same as below.

### 2.3. Biochemical parameter analysis

The blood samples were centrifuged to collect serum, and the serum LPS level was analyzed using the related kit (Xiamen Bioendo Biotechnology, Xiamen, China). After the jejunum tissues were rinsed with normal saline to remove residual feces, the supernatant was collected by centrifugation. The levels of tumor necrosis factor (TNF)- $\alpha$ , interleukin (IL)-1 $\beta$ , IL-6, IL-10, and secretory immunoglobulin A (sIgA) in the jejunum supernatant were analyzed using their respective kits purchased from Elabscience Biotechnology (Wuhan, China). The malondialdehyde (MDA) level and the catalase (CAT), glutathione peroxidase (GSH-Px), and superoxide dismutase (SOD) activities in the supernatant were analyzed using their respective kits purchased from Jiancheng (Nanjing, China) (Wang et al., 2024).

### 2.4. Histopathological analysis

After fixing the jejunum tissues in a paraformaldehyde solution (4 %) for 24 h, they were embedded in a paraffin block, followed by slicing into 5- $\mu$ m-thick slices, dewaxing, and staining with hematoxylin-eosin (H&E) solution or Alcian blue-Periodic acid-Shiff (AB-PAS) solutions (Tian et al., 2023; Zheng et al., 2023). The light microscopy CX31 (Olympus, Tokyo, Japan) was used to photograph.

### 2.5. Analysis of gut microbiota

The total fecal bacterial DNA was extracted, and purified for 16S rRNA sequencing (Qian et al., 2022). The hypervariable V3-V4 regions of the 16S rRNA gene were amplified using 338F and 806R primers and sequenced by Majorbio (Shanghai, China). After sequencing, the raw data were spliced and filtered to obtain the filtered reads, followed by the operational taxonomic units (OTUs) clustering and species classification analysis. The representative sequences for each OTU were annotated using the species information, allowing the retrieval of species-specific details and their corresponding abundance distribution.

### 2.6. Non-targeted metabolomics

Non-targeted metabolomic of the fecal samples (50 mg) was analyzed by Majorbio (Shanghai, China). Multiplicative analyses of variance and the Student's *t*-test were performed. The metabolites with *P*-values < 0.05 and VIP > 1 were considered differential metabolites. Using the KEGG database, the enrichment of differential metabolites in primary biochemical metabolic processes and the signal transduction pathways were investigated.

### 2.7. Immunohistochemistry and immunofluorescence

Immunohistochemistry analysis was performed according to previous work (Tang et al., 2023; Wang et al., 2020). The paraffin-embedded jejunum tissue sections (5  $\mu$ m thick) were incubated with primary antibodies against Claudin-1, Occludin, and ZO-1 overnight, followed by incubation with a biotinylated secondary antibody for 30 min. After counterstaining with DAB concentration kit (DA1010, Solarbio) and hematoxylin, the slides were sealed and photographed under a CX31 biological microscope, and analyzed by Image J 1.52i software. The immunofluorescence experiments were performed as described previously (Chen et al., 2023). The antibodies against the following proteins were used: TLR4, NF- $\kappa$ B p65, p-NF- $\kappa$ B p65, I- $\kappa$ B $\alpha$ , and p-I- $\kappa$ B $\alpha$ .

### 2.8. Statistical analyses

The experimental data was statistically analyzed using SPSS 26.0 and plotted using Origin (Version 2022). The biological data were expressed as mean  $\pm$  standard error of the mean for all the results. The difference with a *P*-value < 0.05 was considered statistically significant.

## 3. Results

### 3.1. DHA-PS alleviated the BPA-induced murine jejunum damage

As shown in Fig. 1B, the morphology and structure of intestinal mucosa in the CON group were unaltered. The intestinal villi were aligned neatly with shallow recesses and clearly visible boundaries. In contrast, the exposure to BPA damaged jejunum morphology, showing the loss of intestinal epithelial integrity, disordered intestinal villi with apical absence, and villi breakage or shedding. Furthermore, the crypt was deep with no obvious boundaries, decreased ratio of intestinal villi length to crypt depth, thinned mucosal muscular layer (Fig. 1D and E). Interestingly, the mice administered with DHA-PS exhibited relatively well-preserved histological morphology with a marked increase in villi length, a decrease in crypt depth, and a marked increase in the ratio of intestinal villi length to crypt depth (Fig. 1D and 1E).

As shown in Fig. 1C, the AB-PAS staining results indicated that goblet cells of the normal jejunum mucosa were round or oval, numerous, clearly visible without obvious defects and loss, and densely distributed in all parts of the villi. However, the mucosal layer of the MOD was significantly damaged with reduced and scattered intestinal mucosal goblet cells in the intestinal villi (Fig. 1F). As compared with MOD, the mucous membrane improved, and the loss of goblet cells decreased in the DHA-PS group. Moreover, the goblet cells number notably increased in both the treatment groups, especially in the 100 DHA-PS (Fig. 1F).

### 3.2. Effect of DHA-PS on intestinal tight junction proteins

In order to explore the intestinal barrier integrity, the expression levels of tight junction protein were determined using immunohistochemistry analysis (Fig. 2). The jejunum tissues of the MOD had considerably lower expression levels of Claudin-1, Occludin, and ZO-1 as compared to those of the CON (*P* < 0.01), suggesting that prolonged exposure to BPA caused damage to the jejunum. As compared to the MOD, the expression levels of tight junction proteins significantly increased after DHA-PS treatment (*P* < 0.01).

### 3.3. Effects of DHA-PS on LPS and sIgA levels

The serum LPS levels in the MOD were considerably higher than those in the CON (Fig. 3A, *P* < 0.01). After DHA-PS treatments, the LPS levels substantially decreased by  $22.93 \pm 0.10$  % (50 DHA-PS) and  $29.27 \pm 0.02$  % (100 DHA-PS) as compared to the MOD, respectively. Moreover, the jejunum sIgA levels were determined to evaluate the integrity and damage degree of the intestinal immune barrier. After BPA treatment, the sIgA levels decreased by  $50.05 \pm 0.07$  % as compared to the CON (Fig. 3B) increased by  $81.07 \pm 0.30$  % (50 DHA-PS) and  $75.92 \pm 0.35$  % (100 DHA-PS) after DHA-PS treatments.

### 3.4. Effects of DHA-PS on the cytokine levels

As seen in Fig. 3C-F, the IL-1 $\beta$ , IL-6, and TNF- $\alpha$  levels were notably higher (*P* < 0.01), while that of IL-10 was notably lower in the jejunum tissues of MOD group as compared to the CON group (*P* < 0.01). Nevertheless, the DHA-PS treatments restored these cytokine levels. Specifically, after the DHA-PS administration (100 mg/kg), the IL-1 $\beta$ , IL-6, and TNF- $\alpha$  levels decreased by  $46.14 \pm 37.93$  %,  $58.40 \pm 3.05$  %, and  $36.51 \pm 0.37$  %, respectively, while the IL-10 levels increased by  $77.41 \pm 16.70$  % as compared to the MOD.

### 3.5. Effects of DHA-PS on oxidative stress indices

As seen in Fig. 3G and 3H, the BPA exposure increased the MDA levels by  $63.20 \pm 0.02$  % as compared to the CON and decreased the CAT, GSH-Px, and SOD activities by  $47.44 \pm 0.05$  %,  $68.13 \pm 2.57$  %, and  $45.47 \pm 0.17$  %, respectively. On the other hand, DHA-PS treatment

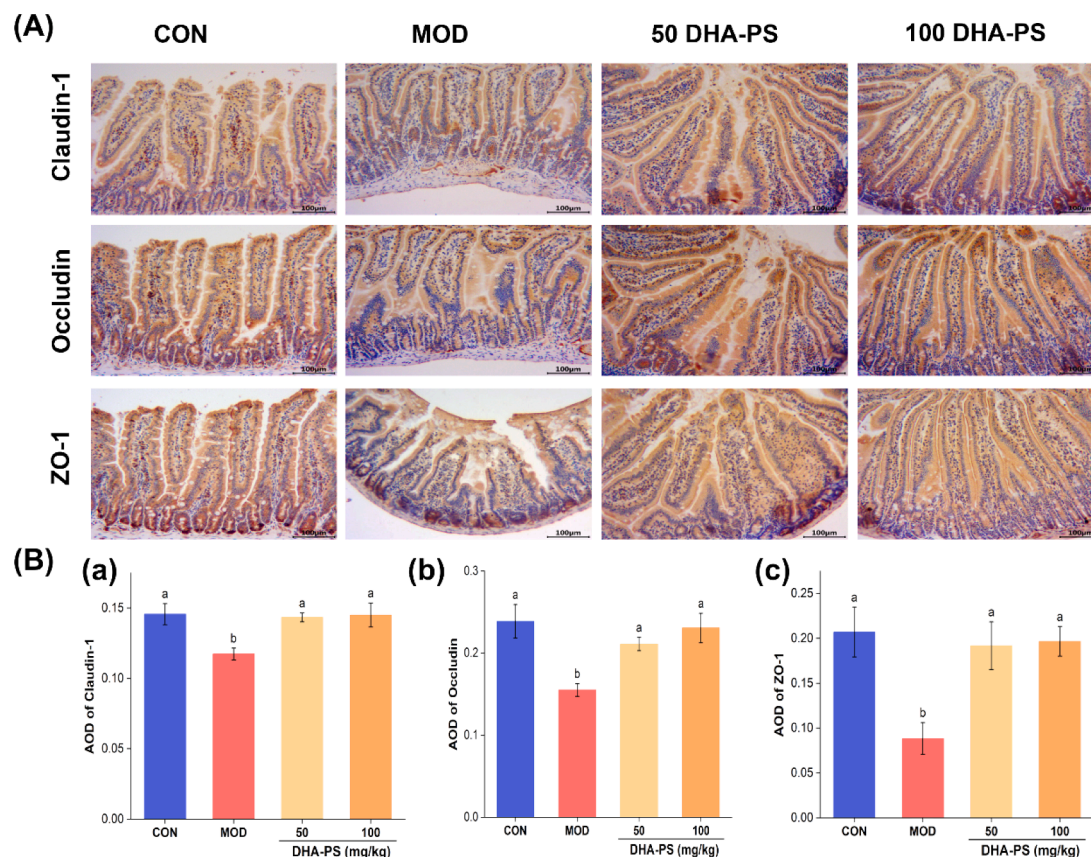


**Fig. 2.** Effect of DHA-PS on BPA-induced intestinal tight junction proteins ( $n = 3$ ). (A) Immunohistochemical analysis ( $200 \times$ ); (B) Quantification average optical density (AOD) values of Claudin-1 (a), Occludin (b), and ZO-1 (c) in the jejunum.

notably decreased MDA levels (Fig. 3G,  $P < 0.01$ ) and increased the CAT, GSH-Px, and SOD activities (Fig. 3H,  $P < 0.01$ ).

### 3.6. Effects of DHA-PS on the murine gut microbiota

The previous results showed that the 100 mg/kg DHA-PS effectively alleviated the BPA-induced intestinal barrier damage. Therefore, the gut microbial composition of the 100 DHA-PS was investigated. A total of 963 OTUs were obtained from all the samples, of which, 532 were common among the three groups. There were 119 unique bacteria in the CON, 42 in the MOD, and 112 in the 100 DHA-PS (Fig. 4A). This indicated that gut microbiota changed after treatment with BPA, which was restored by DHA-PS to the levels of the CON. The rarefaction curves of the Sobs index demonstrated that the sparse curve tended to be flat, indicating that the depth and width of the sequencing samples were sufficient (Fig. 4B). Moreover, as compared to CON, BPA exposure resulted in a decrease in gut microbiota alpha-diversity index (Chao1, Shannon and ACE) and an increase in Simpson index, which was almost restored by the DHA-PS treatment (Supplementary Fig. S1A).

The effects of DHA-PS on the overall structural alterations in gut microbiota were examined using the PCoA and sample hierarchical clustering tree. As shown in Fig. 4C, the principal components (PCs) of the MOD and CON were clearly separated, showing that BPA changed the structure of gut microbiota. In addition, the same phenomena were observed in the hierarchical clustering tree, showing that each of the three groups was clearly separated from each other (Fig. 4D). It was observed that the 100 DHA-PS was closer to the CON than the MOD, indicating that DHA-PS repaired the changes in the structure of gut microbiota.

The structure and composition of gut microbiota at the phylum and

genus levels were examined to compare the effects of BPA and DHA-PS treatments on the gut microbiota. As seen in Fig. 4G, the predominant gut microbial phyla included Firmicutes, Bacteroidota, Verrucomicrobiota, Actinobacteriota, Proteobacteria, Patescibacteria, and Proteobacteria at the phylum level. In comparison to CON, the MOD showed a notable increase in the abundance of Firmicutes, which was reduced by DHA-PS treatment. However, except for Actinobacteriota and Proteobacteria, there were no obvious variations in the relative abundances of other genera among the three groups (Supplementary Fig. S1B). Moreover, the main gut microbiota at the genus level included norank\_f\_Muribaculaceae and *Lactobacillus*, followed by *Akkermansia*, norank\_f\_norank\_o\_Clostridia\_UCG-014, *Lachnospiraceae\_NK4A136\_group*, and *Prevotellaceae\_UCG-001* (Fig. 4H). As compared to the CON, the gut microbiota at the genus level showed a decrease in the abundance of *Coriobacteriaceae\_UCG-002*, *Akkermansia*, *Alistipes*, *Butyrivococcus*, *Enterorhabdus*, and *Lachnospiraceae\_UCG-006* in the MOD compared to the CON (Supplementary Fig. S2). The DHA-PS treatment restored the relative abundances of *Coriobacteriaceae\_UCG-002*, *Akkermansia*, *Alistipes*, *Butyrivococcus*, *Enterorhabdus*, and *Lachnospiraceae\_UCG-006* to normal as compared to the MOD. On the contrary, the abundance of *Desulfovibrio* increased after BPA treatment and was restored by the DHA-PS treatment. Among these different genera, *Faecalibaculum*, *Coriobacteriaceae\_UCG-002*, *Akkermansia*, *Alistipes*, *Butyrivococcus*, and *Lachnospiraceae\_UCG-006* were associated to the short-chain fatty acids (SCFAs) production (Supplementary Fig. S2). Similarly, as compared to the MOD, the heatmap analysis of gut microbiota at the genus level confirmed that the DHA-PS treatment successfully restored their abundance (Supplementary Fig. S1C). Overall, DHA-PS treatment could modulate gut microbiota at the phylum and genus levels.

The diversity of gut microbiota was examined using the multi-level

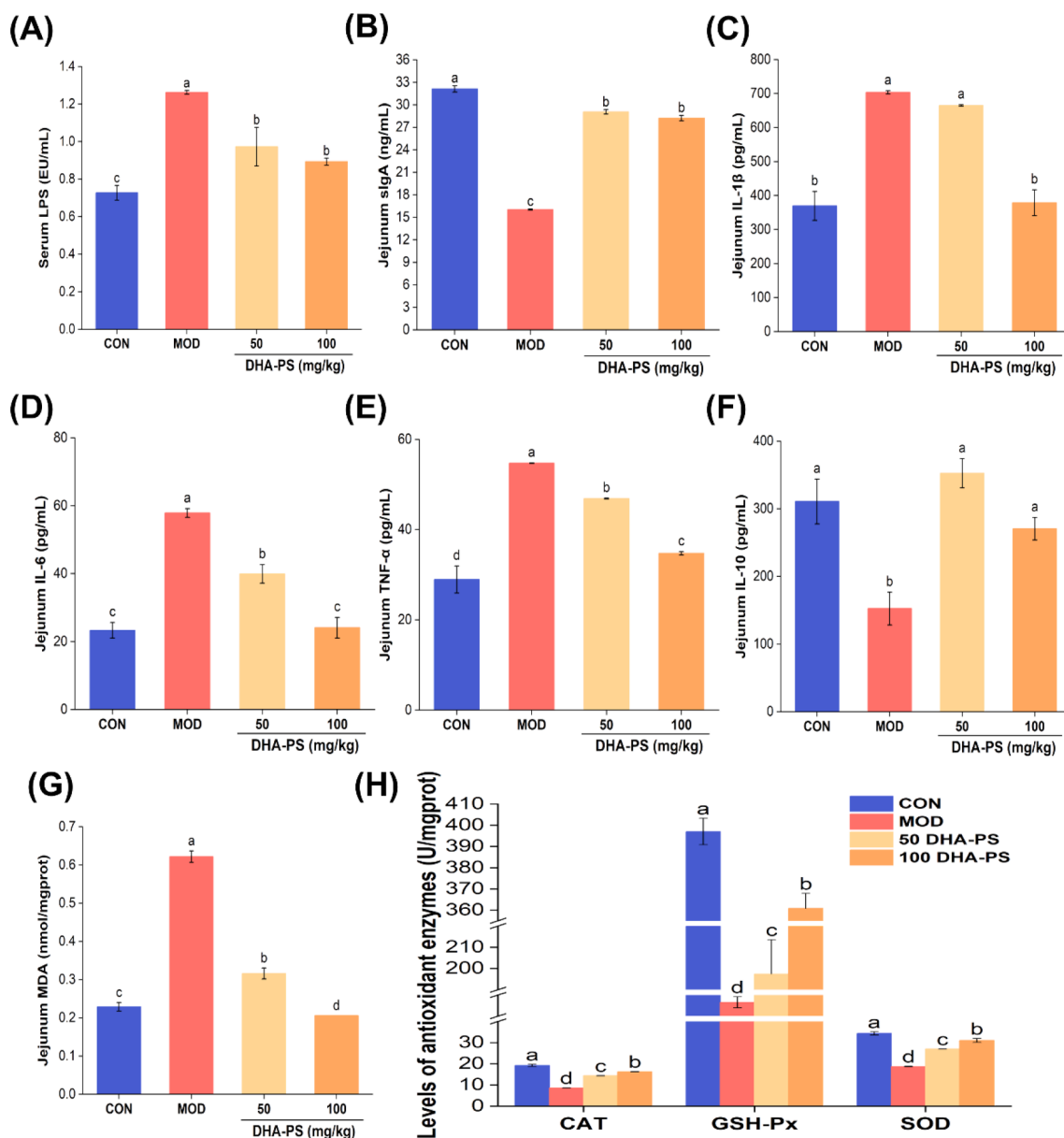


Fig. 3. Effect of DHA-PS on murine biochemical indices ( $n = 6$ ). (A) LPS; (B) sIgA; (C) IL-1 $\beta$ ; (D) IL-6; (E) TNF- $\alpha$ ; (F) IL-10; (G) MDA; (H) CAT, GSH-Px, and SOD.

species hierarchy of LEfSe. The cladogram and LDA histogram (Fig. 4E and 4F) indicated that 24 species exhibited differences in their relative abundances among the three groups, including 17, 2, and 5 species belonging to the CON, MOD, and 100 DHA-PS, respectively. The relative abundances of *Turicibacter*, *Erysipelotrichales*, *Actinobacteriota*, and *Bifidobacteriaceae* were abundant in the CON, while those of unclassified\_f\_Muribaculaceae and *UBA1819* were abundant in the MOD. Moreover, the relative abundances of *Faecalibaculum*, *Harryflintia*, *Negativibacillus*, and *Clostridiaceae* were enriched in the 100 DHA-PS.

Furthermore, PICRUSt was performed to understand the potential role of alterations in the gut microbiota. The top 10 metabolic pathways showing notable differences were as follows: microbial metabolism in diverse environments, carbon metabolism, purine metabolism, cysteine and methionine metabolism, alanine, aspartate, and glutamate metabolism, lysine biosynthesis, propanoate metabolism, carbon fixation in photosynthetic organisms, beta-lactam resistance, and fatty acid metabolism (Supplementary Fig. S1D).

### 3.7. DHA-PS treatment altered metabolomic profiling

As shown in Fig. 5A-D, the results of OPLS-DA models indicated that the gut metabolites were similar within each group but varied between groups, since each group was clearly separated in both the negative and positive modes. The resilience of OPLS-DA models was further demonstrated using the permutation test, which revealed that all the R2 and Q2 values of the models were lower than their starting values (Supplementary Fig. S2A-D). Venn diagram showed that metabolites differed significantly between the groups (Supplementary Fig. S2E). The number of different metabolites shared by the three groups was 26, while 45 were unique to MOD vs CON, 79 were unique to MOD vs 100 DHA-PS, and 411 were unique to CON vs 100 DHA-PS.

The differential metabolites were identified based on parameters  $VIP > 1.0$  and  $P < 0.05$ . A total of 113 differential metabolites were down-regulated and 80 were up-regulated in the MOD as compared to the CON, while 139 were up-regulated and 670 were down-regulated in

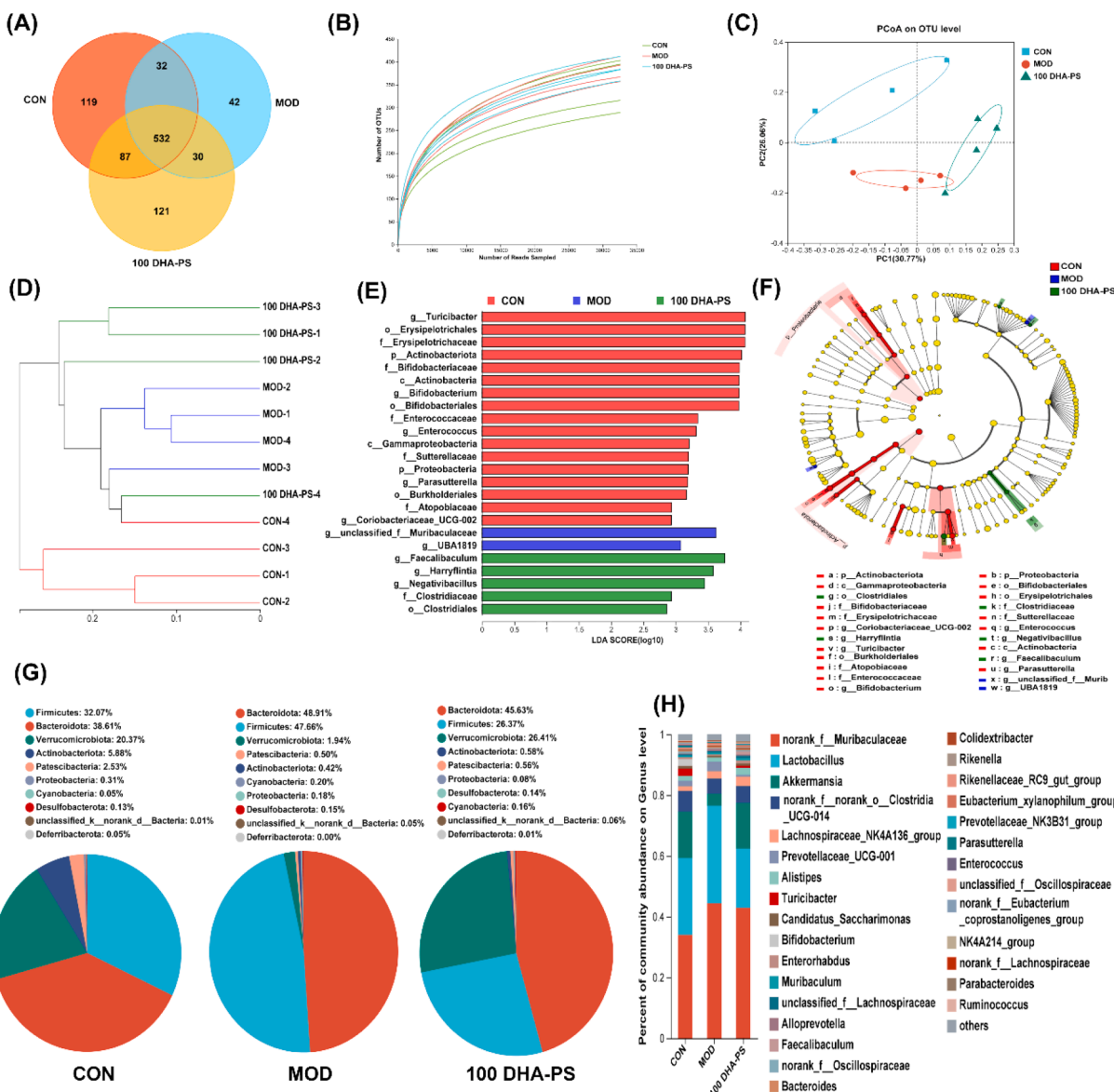


**Fig. 4.** Effects of BPA exposure on gut microbial communities ( $n = 4$ ). (A) Venn diagram of OTUs distribution; (B) Rarefaction curve; (C) PCoA analysis; (D) Hierarchical clustering; (E) LefSe cladogram; (F) LDA value distribution histogram; (G) Gut microbiota composition at phylum level; (H) Gut microbiota composition at genus level.

the 100 DHA-PS as compared to the MOD (Fig. 5E-F). The detected differential metabolites were subjected to a cluster heatmap analysis, and the differences in the top 50 metabolites among the groups are shown in Fig. 6 and Supplementary Tables S1 and S2. Subsequently, the metabolites were categorized based on their involvement in pathways using the KEGG database (Fig. 5G). These metabolites were found to be mainly involved in the following pathways: metabolism, organismal systems, cellular processes, drug development, human diseases, environmental information processing, and genetic information processing. Interestingly, the amino acid and lipid metabolism pathways were notably enriched in the metabolism category (Fig. 5G).

In addition, the significantly altered differential metabolites were further performed using KEGG pathway enrichment analysis to explore the underlying mechanism of DHA-PS improving the murine intestinal barrier. The main metabolic pathways between MOD and CON groups were pyruvate metabolism, phenylalanine metabolism, and biosynthesis of alkaloids derived from ornithine, lysine, nicotinic acid, histidine, and purine (Fig. 5H). The main metabolic pathways of 100 DHA-PS and MOD included arginine and proline metabolism, glycerophospholipid

metabolism, tryptophan metabolism, NF- $\kappa$ B, and MAPK (Fig. 5J). Furthermore, in order to further identify the most influential relevant metabolic pathways, the KEGG enrichment analysis of the top 50 differential metabolites in the 100 DHA-PS vs MOD was performed. The NF- $\kappa$ B pathway was notably enriched and ranked second (Supplementary Fig. S2F).

### 3.8. Effects of DHA-PS on NF- $\kappa$ B pathway

As seen in Fig. 7, as compared to the CON, BPA induced the phosphorylation and nuclear translocation of NF- $\kappa$ B p65 (Fig. 7A), up-regulated the expression levels of TLR4 ( $116.73 \pm 13.90$  vs.  $48.88 \pm 3.88$ ,  $P < 0.01$ ), p-I $\kappa$ B $\alpha$  ( $119.50 \pm 5.12$  vs.  $55.81 \pm 7.42$ ,  $P < 0.01$ ), p-NF- $\kappa$ B p65 ( $80.36 \pm 14.22$  vs.  $61.56 \pm 9.01$ ,  $P < 0.05$ ), and down-regulated that of I $\kappa$ B $\alpha$  ( $41.56 \pm 2.45$  vs.  $135.35 \pm 16.64$ ,  $P < 0.01$ ). However, the DHA-PS treatment reversed the changes in these protein levels in the BPA-induced mice.

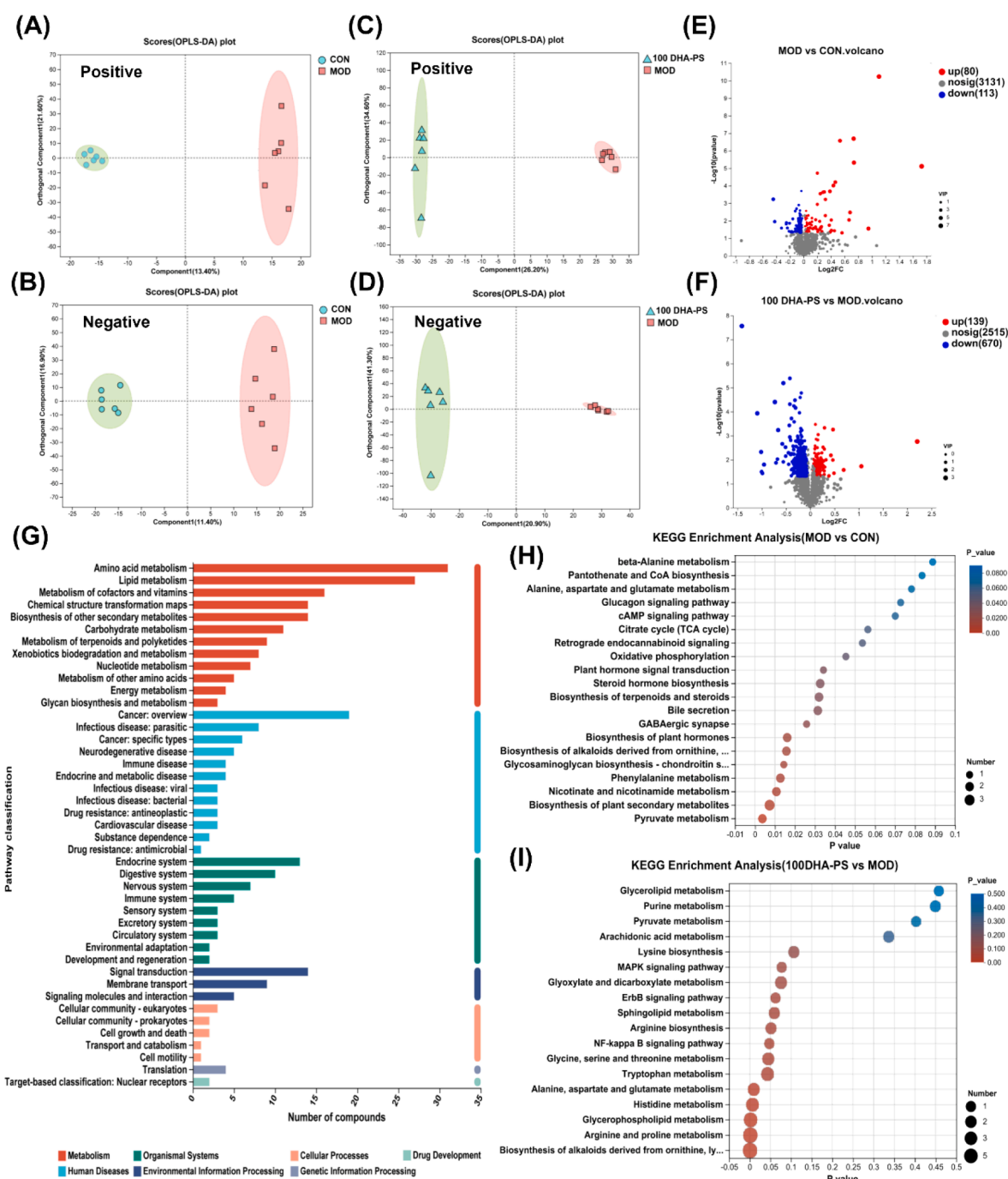


**Fig. 5.** Effect of DHA-PS on metabolome profile ( $n = 6$ ). (A, C): OPLS-DA score plot of the CON and MOD groups in the positive and negative ion; (B, D): OPLS-DA score plot of the 100 DHA-PS and MOD groups in the positive and negative ion; (E, F): Volcanic plots of differential metabolites in the MOD vs CON and DHA-PS vs MOD; (G) KEGG pathway classification; (H) Metabolic pathway enrichment analysis of the MOD vs CON. (I) Metabolic pathway enrichment analysis of the DHA-PS vs MOD.

### 3.9. Correlation analysis

Spearman correlation analysis was further applied to elucidate the relationship between gut microbiota and biological indices. At the phylum level, Actinobacteriota was negatively related to the levels of sIgA, IL-10, and antioxidant enzymes, but positively related to IL-6, TNF- $\alpha$ , and LPS levels (Fig. 8A). Interestingly, Bacteroidota showed the opposite trend. At the genus level, *Gordonibacter*, *Coriobacteriaceae*, UCG-002, and *Turicibacter* were positively related to CAT, SOD, and GSH-Px activities and negatively related to levels of sIgA, IL-6, TNF- $\alpha$ , and LPS, while *norank\_f\_Muribaculaceae* showed the opposite trend

(Fig. 8B).

Spearman correlation analysis was used to elucidate the correlations between 10 biochemical parameters and 20 differential metabolites. A total of 17 metabolites were found to be correlated significantly (Fig. 8C,  $P < 0.05$ ). Interestingly, S-lactoylglutathione and lactucin were positively related to the levels of LPS, IL-1 $\beta$ , IL-6, TNF- $\alpha$ , and MDA but negatively related to the levels of sIgA and IL-10 as well as CAT, SOD, and GSH-Px activities. Specifically, 17-beta-estradiol-3, 17-beta-sulfate, ganoderiol I, cyclopassifloic acid A, allispiroside C, and araliasaponin II belonged to the superclass of lipids and lipid-like molecules.

Spearman correlation analysis was further used to investigate the

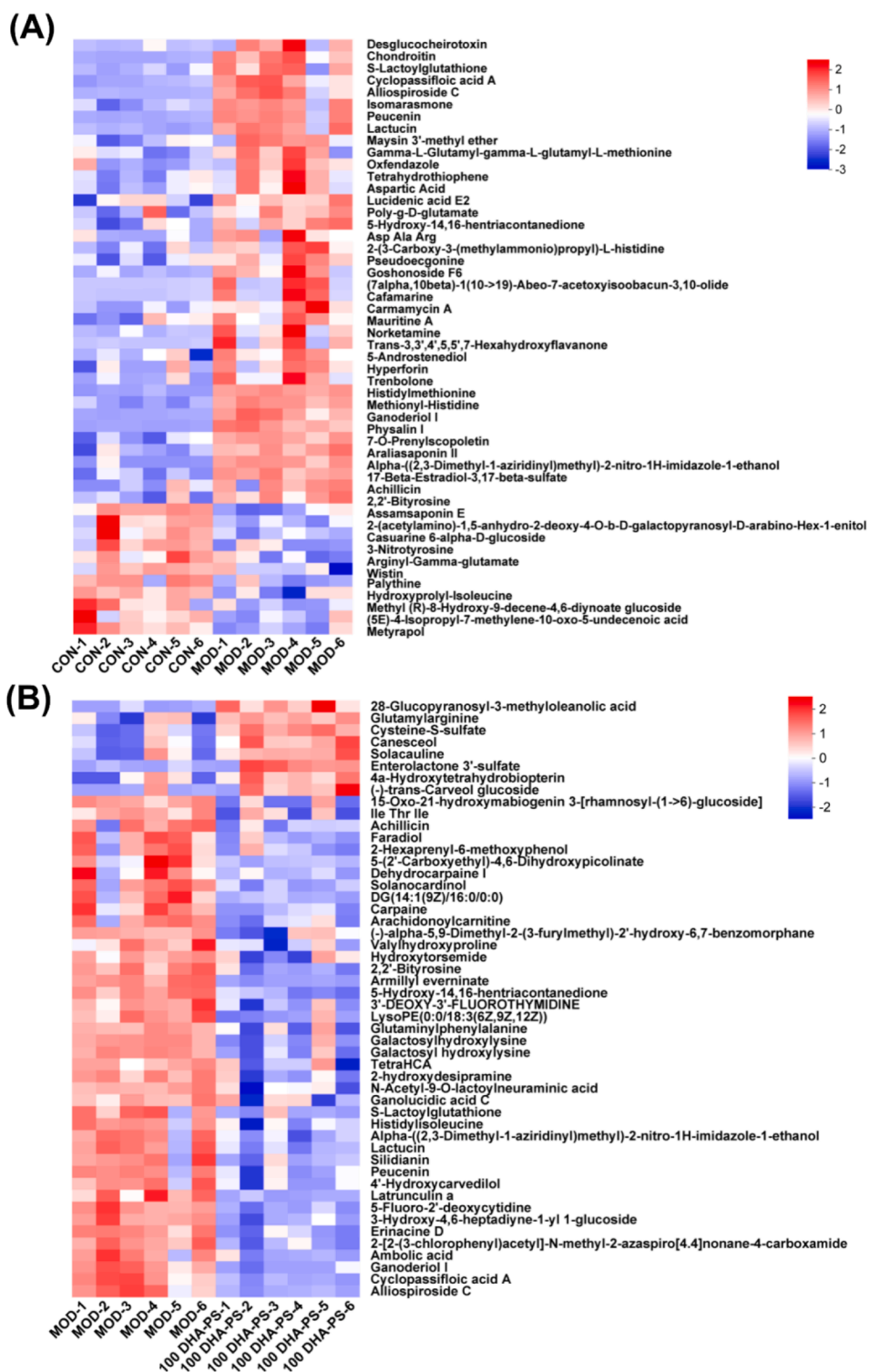


**Fig. 6.** Heat map of the top 50 metabolites ( $n = 6$ ). (A) Heat map of the top 50 metabolites in the MOD vs CON group; (B) Heat map of the top 50 metabolites in the DHA-PS vs MOD group.

relationship between gut microbiota and metabolites after DHA-PS treatment (Fig. 8D). Specifically, genera *Bifidobacterium*, *Parasutterella*, and *Coriobacteriaceae* UCG-002 were positively related to *Cis-p*-menth-2-en-1-ol, annoglabin C, procurcumadiol, deoxynivalenol, cucurbitacin B, and gamma-eudesmol rhamnoside and negatively related to tryptophan glutamate, 4a-hydroxytetrahydrobiopterin, methionyl-

histidine, histidylmethionine, and chondroitin. In contrast, genus *Faecalibaculum* was negatively related to *Cis-p*-Menth-2-en-1-ol, annoglabin C, procurcumadiol, deoxynivalenol, cucurbitacin B, and gamma-eudesmol rhamnoside, which belonged to the superclass of lipids and lipid-like molecules.

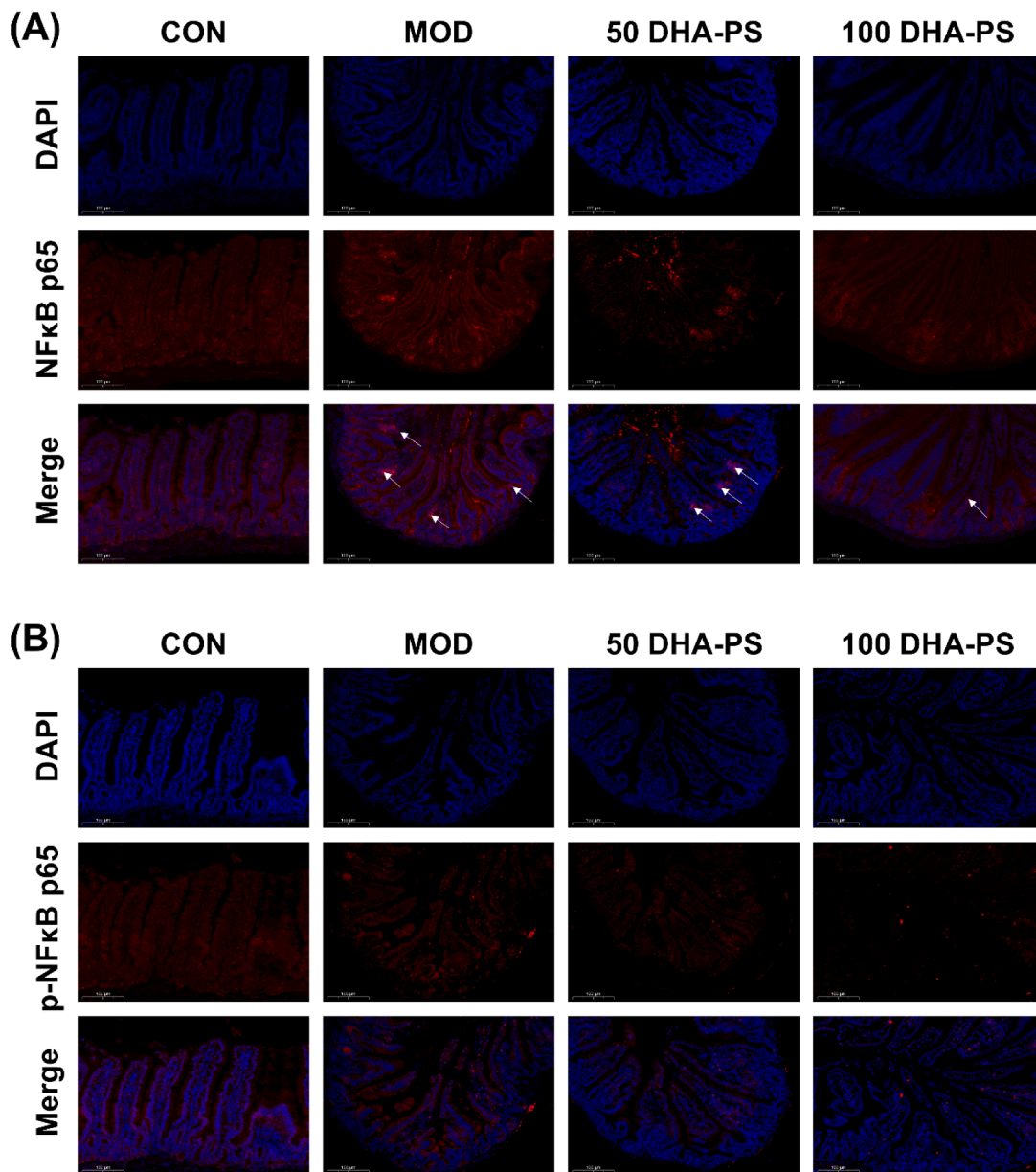


**Fig. 7.** Effects of DHA-PS on NF- $\kappa$ B pathway. (A-C) Representative images of the expression of TLR4, I $\kappa$ B $\alpha$ , p-I $\kappa$ B $\alpha$ , NF- $\kappa$ B p65 and p-NF- $\kappa$ B p65 in four groups ( $n = 3$ ); (D) Fluorescence intensity of mean immunofluorescence staining. The white arrow showed the translocation of NF- $\kappa$ B p65. TLR4, I $\kappa$ B $\alpha$ , p-I $\kappa$ B $\alpha$ , NF- $\kappa$ B p65 and p-NF- $\kappa$ B p65 (red), DAPI (blue), scale bar = 100  $\mu$ m.

#### 4. Discussion

The human intestine is the largest digestive organ, where the most important part of the digestive process occurs (Ber et al., 2021). Numerous studies have indicated that prolonged exposure to BPA has detrimental effects on intestinal health, such as dysfunction of intestinal mucosal homeostasis and gut microbiota as well as enhanced susceptibility to inflammatory bowel disease (IBD) (Feng et al., 2019; Yao et al., 2023b). Therefore, researchers have paid more attention to the BPA-induced intestinal dysfunction and are actively searching for strategies to alleviate this dysfunction. A previous study demonstrated that DHA-PS improved the HFD-induced murine jejunum damage and effectively regulated the dysfunction of gut microbiota (Tian et al., 2023). Therefore, the protective effects of DHA-PS on BPA-induced intestinal damage are worthy to be studied.

The intestinal barrier is a key factor to prevent intestinal pathogenic

microorganisms and harmful substances from entering the body and endangering the host's health (Wang et al., 2022). It is mainly composed of physical, chemical, microbial, and immune barriers (Gonzalez-Correa et al., 2017). The physical barrier maintains the selective permeability of intestinal epithelium by regulating paracellular and extracellular pathways, while the chemical barrier is formed of mucin secreted by goblet cells (Grondin et al., 2020). The immune barrier is formed by the secretion of cytokines, immunoglobulin, and antimicrobial peptides, which shield the host against infection (Rescigno, 2011). In this study, the proportion of goblet cells and the levels of Claudin-1, Occludin, ZO-1, sIgA, and IL-10 notably decreased, while the IL-1 $\beta$ , IL-6, and TNF- $\alpha$  levels notably increased in the MOD. This demonstrated that long-term exposure to BPA caused intestinal barrier dysfunction (Wang, et al., 2021). However, DHA-PS alleviated the BPA-induced jejunum damage by notably increasing the proportion of goblet cells and levels of Claudin-1, Occludin, ZO-1, sIgA, and IL-10 while decreasing the levels of

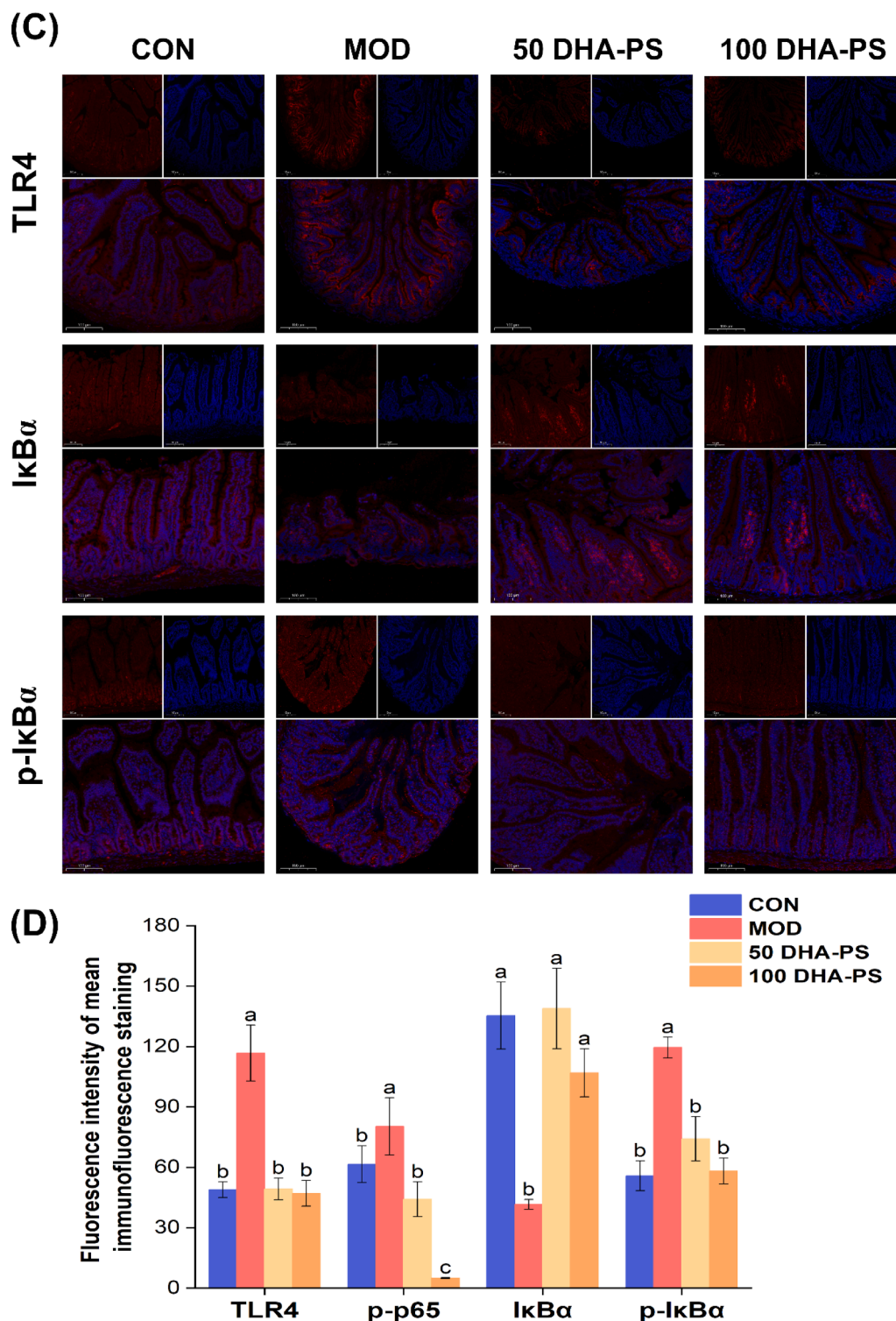


Fig. 7. (continued).

proinflammatory factor; this was consistent with our previous study (Tian et al., 2023).

A recent study demonstrated that BPA exposure could disrupt redox homeostasis and induce oxidative stress in the body (Mueller et al., 2018). In addition, intestinal inflammation can commonly stimulate other immune cells and trigger T-cell reactions through the immune system, further causing oxidative damage to the intestine (Yang et al., 2023). In this study, the BPA exposure decreased the CAT, SOD, and GSH-Px activities and increased the MDA, IL-1 $\beta$ , IL-6, and TNF- $\alpha$  levels

in the jejunum tissues, indicating the imbalance of oxidative status in the jejunum. In this study, DHA-PS treatment alleviated the BPA-induced jejunum damage by inhibiting oxidative, which was consistent with previous researches (Cao et al., 2019; Che et al., 2021).

Gut microbiota performs various physiological functions, including immune, metabolic, and endocrine functions, and plays vital roles in maintaining host health (Buffie & Pamer, 2013). Researches have reported that BPA can affect the composition of gut microbiota (Feng et al., 2020; Lai et al., 2016). This study confirmed that BPA exposure

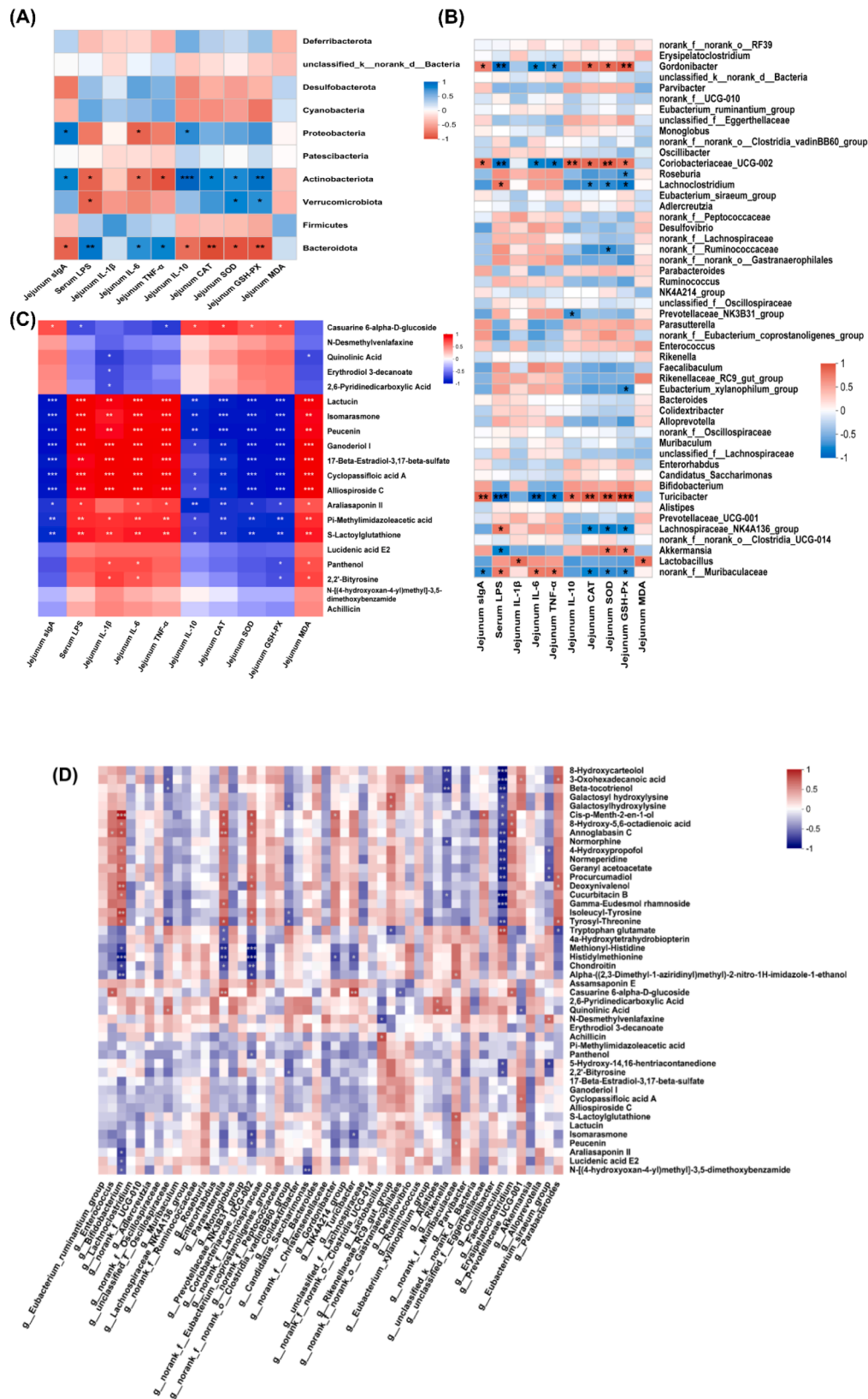


**Fig. 8.** Correlation analysis amongst biochemical parameters, microbiome and metabolome. (A) Spearman's correlation of biochemical parameters and gut microbiota at phylum level. (B) Spearman's correlation of biochemical parameters and gut microbiota at genus level. (C) Spearman's correlation of biochemical parameters and differential metabolites. (D) Spearman's correlation between gut microbiota and differential metabolites at genus level. \*  $P < 0.05$ , \*\*  $P < 0.01$  and \*\*\*  $P < 0.001$  indicated significant correlation.

caused the dysbiosis of gut microbiota with a change in  $\alpha$ -diversity and  $\beta$ -diversity; this result was consistent with previous studies (Feng et al., 2020; Lai et al., 2016). Nevertheless, the relative abundance of certain bacterial taxa also changed, and Bacteroidetes and Firmicutes became the dominant phyla in the MOD, accounting for more than 90 % of the total gut microbial species, which was similar with a previous study by Liu et al. (Liu et al., 2022). However, the DHA-PS treatment increased the ACE, Chao, and Shannon indices and decreased the Simpson index, showing that DHA-PS could effectively reverse the BPA-induced decrease in  $\alpha$ -diversity. Similarly, the  $\beta$ -diversity analysis and hierarchical cluster analysis suggested that BPA could significantly alter the composition of gut microbiota, which was reversed by DHA-PS.

Gram-positive bacteria known as Actinobacteria play critical roles in keeping the homeostasis of the intestinal barrier (Binda et al., 2018). However, Bacteroides, the proinflammatory bacteria, are correlated with IBD (Takayama et al., 2021). A clinical study showed that in patients with IBD, the abundance of Actinobacteria decreased, while that of *Bacteroides* increased (Alam et al., 2020); this was consistent with the current study results. The administration of DHA-PS reversed this trend, and the correlation analysis showed that Actinobacteria was negatively associated with sIgA, IL-10, and antioxidant enzymes, and positively associated with IL-6, TNF- $\alpha$  and LPS levels, while Bacteroides showed the opposite trend.

SCFAs are created by gut microbiota through the fermentation of undigested carbohydrates, such as butyric, propionic, and acetic acids (Yue et al., 2023). In this study, DHA-PS treatment significantly improved the relative abundances of beneficial bacterial genera, including *Akkermansia*, *Alistipes*, *Butyricoccus*, *Coriobacteriaceae*\_UCG-002, *Enterorhabdus*, and *Lachnospiraceae*\_UCG-006 and decreased that of harmful bacteria (*Desulfovibrio*). Interestingly, the majority of these beneficial bacteria are related to the production of SCFAs (Deng et al., 2023; Wang et al., 2023). However, the harmful bacterial genus *Desulfovibrio* might degrade SCFAs and amino acids, producing hydrogen sulfide, which could damage intestinal epithelial cells in mice (Wei et al., 2023). *Akkermansia*, as a probiotic in gut microbiota, could improve the intestinal barrier and inhibit inflammation by elevating the expressions of tight junction protein in C57BL/6 mice (Chelakkot et al., 2018). In addition, *Alistipes*, *Butyricoccus*, *Coriobacteriaceae*\_UCG-002, and *Lachnospiraceae*\_UCG-006 are also SCFA-producing bacteria (Li et al., 2023; Wang et al., 2023). The functional mechanism analysis of gut microbiota also showed the relationship between gut microbiota and propanoate metabolism. Taken together, DHA-PS could alleviate intestinal inflammatory damage by regulating gut microbiota.

Gut microbial metabolites play vital roles in maintaining gut health and homeostasis (Belizário et al., 2018). Tryptophan is involved in regulating immune response, oxidative stress, and inflammation (Anesi et al., 2019). Only a minor portion of tryptophan is metabolized via the serotonin pathway, while the rest is transformed via the kynurenine and indole pathways (Chen et al., 2022). Notably, both the LPS and inflammatory cytokines can activate indoleamine 2, 3-dioxygenase 1 and promote tryptophan metabolism through the kynurenine pathway (Fujigaki et al., 2001; Liu et al., 2015). In this study, DHA-PS inhibited the kynurenine pathway of tryptophan metabolism, thereby increasing the levels of tryptophan and finally inhibiting intestinal inflammation.

Tryptophan, phenylalanine, and tyrosine are aromatic amino acids that are essential for biological metabolism by synthesizing reductive chemicals, thereby maintaining cell redox status in equilibrium (Aon et al., 2020). Glutaminyphenylalanine and 2, 2'-bityrosine are mainly associated with phenylalanine metabolism. Previous studies demonstrated a marked increase in the serum levels of tyrosine and phenylalanine in diabetic rats, showing their potential role as biomarkers of the disease. In this study, the correlation analysis of various lipids and lipid-like molecules (such as 17-beta-estradiol-3, 17-beta-sulfate, ganoderiol I, cyclopassifloic acid A, alliospiroside, and caraliasaponin II) with physiological indices demonstrated their positive correlation with IL-1 $\beta$ , IL-6, and TNF- $\alpha$ , and serum LPS levels and negative correlation with

antioxidant enzymes and IL-10. Among all the emphasized lipid molecules, it was worth noting that arachidonoylcarnitine was related to the arachidonic acid metabolism, a precursor to eicosanoids and prostaglandins that mediate a range of reactions causing inflammation and mitochondrial dysfunction (Natarajan et al., 2010). Interestingly, the DHA-PS treatment decreased the arachidonoylcarnitine contents, indicating that DHA-PS could improve arachidonic acid metabolism by down-regulating arachidonoylcarnitine.

The KEGG enrichment analysis of the top 50 differential metabolites with the highest influence suggested that the NF- $\kappa$ B was the most influential pathway. In addition, structural alterations in gut microbiota could cause an imbalance in bacterial dynamics and elevate the abundance of Gram-negative bacteria, thereby leading to produce endotoxins (Zhang et al., 2022). The breakdown of the intestinal barrier increases intestinal permeability, which further increases the risk of LPS entering the bloodstream (Ye et al., 2021). Moreover, the high levels of endotoxin bind to TLR4 and activate the NF- $\kappa$ B pathway, which leads to the production of various inflammatory mediators and cytokines, thereby promoting apoptosis, increasing intestinal permeability, and accelerating the occurrence of intestinal diseases (Chen et al., 2022; Zhao et al., 2023). In this study, exposure to BPA could break down the intestinal tight junctions and increase intestinal permeability. However, DHA-PS treatment decreased the serum LPS levels and restrained the LPS-mediated TLR4/NF- $\kappa$ B pathway.

## 5. Conclusions

Overall, the current study suggested that DHA-PS could alleviate the BPA-induced intestinal damage. Specifically, the beneficial effects of DHA-PS might be through relieving oxidative stress and inflammation, regulating the imbalance of gut microbiota, increasing tight junction protein expressions, and enhancing intestinal barrier function, thus reducing the leakage of LPS into the bloodstream and restraining LPS/TLR4/NF- $\kappa$ B pathway. In addition, DHA-PS treatment elevated the level of tryptophan and regulated lipid and arachidonic acid metabolism, further improving BPA-induced intestinal damage. Nevertheless, the metabolism and absorption of DHA-PS, and the other molecular forms of DHA/EPA need to be further studied in the future.

## Ethics statement

All the animal protocols were approved by the Animal Ethics Committee of Zhejiang Ocean University (certificate no. 2022021).

## CRediT authorship contribution statement

**Qiaoling Zhao:** Writing – review & editing, Funding acquisition, Formal analysis, Data curation, Conceptualization. **Fei Yang:** Formal analysis, Data curation. **Qiuyan Pu:** Project administration, Methodology, Investigation, Formal analysis, Data curation. **Rui Zhao:** Methodology, Investigation, Formal analysis, Data curation. **Su Jiang:** Formal analysis, Data curation. **Yunping Tang:** Writing – review & editing, Supervision, Funding acquisition, Conceptualization.

## Declaration of competing interest

The authors declare that they have no known competing financial interests or personal relationships that could have appeared to influence the work reported in this paper.

## Data availability

Data will be made available on request.

## Acknowledgments

This work was financially supported by the Eyas Program Incubation Project of Zhejiang Provincial Administration for Market Regulation (No. CY2023329), Medical Health Science and Technology Project of Hangzhou Health Commission (No. A20210366), Zhejiang Provincial Medical and Health Science and Technology Project (No. 2022RC062), and Zhoushan Science and Technology Project (No.2022C41004).

## Appendix A. Supplementary material

Supplementary data to this article can be found online at <https://doi.org/10.1016/j.jff.2024.106229>.

## References

- Alam, M. T., Amos, G. C. A., Murphy, A. R. J., Murch, S., Wellington, E. M. H., & Arasaradnam, R. P. (2020). Microbial imbalance in inflammatory bowel disease patients at different taxonomic levels. *Gut Pathogens*, *12*, 1.
- Almeida, S., Raposo, A., Almeida-Gonzalez, M., & Carrascosa, C. (2018). Bisphenol A: Food exposure and impact on human health. *Comprehensive Reviews in Food Science and Food Safety*, *17*, 1503–1517.
- Anesi, A., Rubert, J., Oluwagbemigun, K., Orozco-Ruiz, X., Nöthlings, U., Breteler, M. M. B., & Mattivi, F. (2019). Metabolic profiling of human plasma and urine, targeting tryptophan, tyrosine and branched chain amino acid pathways. *Metabolites*, *9*, 261.
- Aon, M. A., Bernier, M., Mitchell, S. J., Di Germanio, C., Mattison, J. A., Ehrlich, M. R., & de Cabo, R. (2020). Untangling determinants of enhanced health and lifespan through a multi-omics approach in mice. *Cell Metabolism*, *32*, 100–116.e4.
- Belizário, J. E., Faintuch, J., & Garay-Malpartida, M. (2018). Gut microbiome dysbiosis and immunometabolism: New frontiers for treatment of metabolic diseases. *Mediators of Inflammation*, *2018*, 2037838.
- Ber, Y., Garcia-Lopez, S., Gargallo-Puyuelo, C. J., & Gomollon, F. (2021). Small and large intestine (II): Inflammatory bowel disease, short bowel syndrome, and malignant tumors of the digestive tract. *Nutrients*, *13*, 2325.
- Binda, C., Lopetuso, L. R., Rizzatti, G., Gibiino, G., Cennamo, V., & Gasbarrini, A. (2018). Actinobacteria: A relevant minority for the maintenance of gut homeostasis. *Digestive and Liver Disease*, *50*, 421–428.
- Buffie, C. G., & Pamer, E. G. (2013). Microbiota-mediated colonization resistance against intestinal pathogens. *Nature Reviews Immunology*, *13*, 790–801.
- Camilleri, M., Madsen, K., Spiller, R., Van Meerveld, B. G., & Verne, G. N. (2012). Intestinal barrier function in health and gastrointestinal disease. *Neurogastroenterology & Motility*, *24*, 503–512.
- Cao, W. X., Wang, C. C., Chin, Y. X., Chen, X., Gao, Y., Yuan, S. H., & Tang, Q. J. (2019). DHA-phospholipids (DHA-PL) and EPA-phospholipids (EPA-PL) prevent intestinal dysfunction induced by chronic stress. *Food & Function*, *10*, 277–288.
- Che, H. X., Li, H. Y., Song, L., Dong, X. F., Yang, X. H., Zhang, T. T., & Xie, W. C. (2021). Orally administered DHA-enriched phospholipids and DHA-enriched triglyceride relieve oxidative stress, improve intestinal barrier, modulate inflammatory cytokine and gut microbiota, and meliorate inflammatory responses in the brain in dextran sodium sulfate induced colitis in mice. *Molecular Nutrition & Food Research*, *65*, 2000986.
- Chelakkot, C., Choi, Y., Kim, D. K., Park, H. T., Ghim, J., Kwon, Y., & Ryu, S. H. (2018). Akkermansia muciniphila-derived extracellular vesicles influence gut permeability through the regulation of tight junctions. *Experimental & Molecular Medicine*, *50*, e450.
- Chen, J. M., Wang, M. C., Zhang, P., Li, H., Qu, K., Xu, R. M., & Zhu, H. B. (2022). Cordycepin alleviated metabolic inflammation in Western diet-fed mice by targeting intestinal barrier integrity and intestinal flora. *Pharmacological Research*, *178*, Article 106191.
- Chen, J. Z., Vitetta, L., Henson, J. D., & Hall, S. (2022). Intestinal dysbiosis, the tryptophan pathway and nonalcoholic steatohepatitis. *International Journal of Tryptophan Research*, *15*, 11786469211070533.
- Chen, Y. J., Zhang, M., Li, S. S., Wang, W., Wang, Y. P., & Yin, C. H. (2023). Exposure to bisphenol A induces abnormal fetal heart development by promoting ferroptosis. *Ecotoxicology and Environmental Safety*, *255*, Article 114753.
- Deng, Y. J., Wang, R. D., Li, X. P., Tan, X. Q., Zhang, Y. H., Gooneratne, R., & Li, J. R. (2023). Fish oil ameliorates vibrio parahaemolyticus infection in mice by restoring colonic microbiota, metabolic profiles, and immune homeostasis. *Journal of Agricultural and Food Chemistry*, *71*, 6920–6934.
- Du, L., Hao, Y. M., Yang, Y. H., Zheng, Y., Wu, Z. J., Zhou, M. Q., & Su, G. H. (2022). DHA-enriched phospholipids and EPA-enriched phospholipids alleviate lipopolysaccharide-induced intestinal barrier injury in mice via a Sirtuin 1-dependent mechanism. *Journal of Agricultural and Food Chemistry*, *70*, 2911–2922.
- Feng, D., Zhang, H. M., Jiang, X., Zou, J., Li, Q. R., Mai, H. Y., & Feng, X. (2020). Bisphenol A exposure induces gut microbiota dysbiosis and consequent activation of gut-liver axis leading to hepatic steatosis in CD-1 mice. *Environmental Pollution*, *265*, Article 114880.
- Feng, L., Chen, S. J., Zhang, L. J., Qu, W., & Chen, Z. G. (2019). Bisphenol A increases intestinal permeability through disrupting intestinal barrier function in mice. *Environmental Pollution*, *254*, Article 112960.
- Fujigaki, S., Saito, K., Sekikawa, K., Tone, S., Takikawa, O., Fujii, H., & Seishima, M. (2001). Lipopolysaccharide induction of indoleamine 2,3-dioxygenase is mediated dominantly by an IFN- $\gamma$ -independent mechanism. *European Journal of Immunology*, *31*, 2313–2318.
- Garrett, W. S., Gordon, J. I., & Glimcher, L. H. (2010). Homeostasis and Inflammation in the Intestine. *Cell*, *140*, 859–870.
- Gonzalez-Correa, C. A., Mulett-Vasquez, E., Miranda, D. A., Gonzalez-Correa, C. H., & Gomez-Buitrago, P. A. (2017). The colon revisited or the key to wellness, health and disease. *Medical Hypotheses*, *108*, 133–143.
- Grondin, J. A., Kwon, Y. H., Far, P. M., Haq, S., & Khan, W. I. (2020). Mucins in intestinal mucosal defense and inflammation: Learning from clinical and experimental studies. *Frontiers in Immunology*, *11*, 2054.
- Groschwitz, K. R., & Hogan, S. P. (2009). Intestinal barrier function: Molecular regulation and disease pathogenesis. *Journal of Allergy and Clinical Immunology*, *124*, 3–20.
- Lai, K. P., Chung, Y. T., Li, R., Wan, H. T., & Wong, C. K. C. (2016). Bisphenol A alters gut microbiome: Comparative metagenomics analysis. *Environmental Pollution*, *218*, 923–930.
- Li, L., Wang, C. C., Jiang, S., Li, R., Zhang, T. T., Xue, C. H., Yanagita, T., Jiang, X. M., & Wang, Y. M. (2022). The absorption kinetics of Antarctic krill oil phospholipid liposome in blood and the digestive tract of healthy mice by single gavage. *Food Science and Human Wellness*, *9*, 88–94.
- Li, Q., Liu, W. J., Zhang, H., Chen, C., Liu, R. H., Hou, H. W., & Zhu, W. F. (2023).  $\alpha$ -D-1,3-glucan from *Radix Puerariae thomsonii* improves NAFLD by regulating the intestinal flora and metabolites. *Carbohydrate Polymers*, *299*, Article 120197.
- Liu, J. J., Raynal, S., Bailbé, D., Gausseres, B., Carbonne, C., Autier, V., ... Portha, B. (2015). Expression of the kynurenine pathway enzymes in the pancreatic islet cells. Activation by cytokines and glucolipotoxicity. *Biochimica et Biophysica Acta (BBA) - Molecular Basis of Disease*, *1852*, 980–991.
- Liu, Y. J., Zhang, Q., Guo, Y. L., Liu, J. Y., Xu, J., Li, Z. J., Wang, J. F., Wang, Y. M., & Xue, C. H. (2017). Enzymatic synthesis of lysophosphatidylcholine with n-3 polyunsaturated fatty acid from sn-glycero-3-phosphatidylcholine in a solvent-free system. *Food Chemistry*, *226*, 165–170.
- Liu, R. J., Cai, D. B., Li, X. S., Liu, B. P., Chen, J. L., Jiang, X. W., & Jin, Y. L. (2022). Effects of bisphenol A on reproductive toxicity and gut microbiota dysbiosis in male rats. *Ecotoxicology and Environmental Safety*, *239*, Article 113623.
- Ma, Y., Liu, H. H., Wu, J. X., Yuan, L., Wang, Y. Q., Du, X. D., & Zhang, H. Z. (2019). The adverse health effects of bisphenol A and related toxicity mechanisms. *Environmental Research*, *176*, Article 108575.
- Mueller, S. G., Jardim, N. S., Quines, C. B., & Nogueira, C. W. (2018). Diphenyl diselenide regulates Nrf2/Keap-1 signaling pathway and counteracts hepatic oxidative stress induced by bisphenol A in male mice. *Environmental Research*, *164*, 280–287.
- Natarajan, S. K., Thangaraj, K. R., Eapen, C. E., Ramachandran, A., Mukhopadhyay, A., Mathai, M., & Balasubramanian, K. A. (2010). Liver injury in acute fatty liver of pregnancy: Possible link to placental mitochondrial dysfunction and oxidative stress. *Hepatology*, *51*, 191–200.
- Pu, Q. Y., Yang, F., Zhao, R., Jiang, S., Tang, Y. P., & Han, T. (2023). Investigation of the potential ameliorative effects of DHA-enriched phosphatidylserine on bisphenol A-induced murine nephrotoxicity. *Food and Chemical Toxicology*, *180*, Article 114012.
- Qian, L., Tian, S. S., Jiang, S., Tang, Y. P., & Han, T. (2022). DHA-enriched phosphatidylcholine from *Clupea harengus* roes regulates the gut-liver axis to ameliorate high-fat diet-induced non-alcoholic fatty liver disease. *Food & Function*, *13*, 11555–11567.
- Rescigno, M. (2011). The intestinal epithelial barrier in the control of homeostasis and immunity. *Trends in Immunology*, *32*, 256–264.
- Sartor, R. B. (2008). Microbial influences in inflammatory bowel diseases. *Gastroenterology*, *134*, 577–594.
- Song, S. M., Duan, Y. S., Zhang, T., Zhang, B., Zhao, Z., Bai, X. Y., & Sun, H. W. (2019). Serum concentrations of bisphenol A and its alternatives in elderly population living around e-waste recycling facilities in China: Associations with fasting blood glucose. *Ecotoxicology and Environmental Safety*, *169*, 822–828.
- Takayama, S., Katada, K., Takagi, T., Iida, T., Ueda, T., Mizushima, K., & Naito, Y. (2021). Partially hydrolyzed guar gum attenuates non-alcoholic fatty liver disease in mice through the gut-liver axis. *World Journal of Gastroenterology*, *27*, 2160–2176.
- Tang, Y. P., Zhao, R., Pu, Q. Y., Jiang, S., Yu, F. M., Yang, Z. S., & Han, T. (2023). Investigation of nephrotoxicity on mice exposed to polystyrene nanoplastics and the potential amelioration effects of DHA-enriched phosphatidylserine. *Science of the Total Environment*, *892*, Article 164808.
- Tian, S. S., Zhao, Y. F., Qian, L., Jiang, S., Tang, Y. P., & Han, T. (2023). DHA-enriched phosphatidylserine alleviates high fat diet-induced jejunum injury in mice by modulating gut microbiota. *Food & Function*, *14*, 1415–1429.
- Wang, C. C., Shi, H. H., Xu, J., Yanagita, T., Xue, C. H., Zhang, T. T., & Wang, Y. M. (2020). Docosahexaenoic acid-acylated astaxanthin ester exhibits superior performance over non-esterified astaxanthin in preventing behavioral deficits coupled with apoptosis in MPTP-induced mice with Parkinson's disease. *Food Function*, *11*, 8038–8050.
- Wang, H. D., Chen, H. H., Lin, Y. Y., Wang, G., Luo, Y. Q., Li, X. Y., & Barri, A. (2022). Butyrate glycerides protect against intestinal inflammation and barrier dysfunction in mice. *Nutrients*, *14*, 3991.
- Wang, H., Shen, Q., Fu, Y. X., Liu, Z. Y., Wu, T., Wang, C., & Zhao, Q. Y. (2023). Effects on diabetic mice of consuming lipid extracted from Foxtail Millet (*Setaria italica*): Gut microbiota analysis and serum metabolomics. *Journal of Agricultural and Food Chemistry*, *71*, 10075–10086.
- Wang, K., Qiu, L., Zhu, J. J., Sun, Q., Qu, W., Yu, Y. F., & Shao, G. Y. (2021). Environmental contaminant BPA causes intestinal damage by disrupting cellular

- repair and injury homeostasis in vivo and in vitro. *Biomedicine & Pharmacotherapy*, 137, Article 111270.
- Wang, Q., Xu, K. J., Cai, X., Wang, C. J., Cao, Y., & Xiao, J. (2023). Rosmarinic acid restores colonic mucus secretion in colitis mice by regulating gut microbiota-derived metabolites and the activation of inflammasomes. *Journal of Agricultural and Food Chemistry*, 71, 4571–4585.
- Wei, X., Cheng, F. E., Liu, J. Y., Cheng, Y. F., Yun, S. J., Meng, J. L., & Feng, C. P. (2023). *Sparassis latifolia* polysaccharides inhibit colon cancer in mice by modulating gut microbiota and metabolism. *International Journal of Biological Macromolecules*, 232, Article 123299.
- Wang, Z., Fang, Y., Zeng, Y., Yang, X., Yu, F. M., & Wang, B. (2024). Immunomodulatory peptides from thick-shelled mussel (*Mytilus coruscus*): Isolation, identification, molecular docking and immunomodulatory effects on RAW264.7 cells. *Food Bioscience*, 59, Article 103874.
- Yang, Q., Liu, J. B., Li, T., Lyu, S., Liu, X. T., Du, Z. Y., & Zhang, T. (2023). Integrated microbiome and metabolomic analysis reveal the repair mechanisms of ovalbumin on the intestine barrier of colitis mice. *Journal of Agricultural and Food Chemistry*, 71, 8894–8905.
- Yao, Y. J., Chen, T., Wu, H., Yang, N. X., & Xu, S. W. (2023). Melatonin attenuates bisphenol A-induced colon injury by dual targeting mitochondrial dynamics and Nrf2 antioxidant system via activation of SIRT1/PGC-1 alpha signaling pathway. *Free Radical Biology and Medicine*, 195, 13–22.
- Yao, Y. J., Zhu, W. J., Han, D. X., Shi, X., & Xu, S. W. (2023). New insights into how melatonin ameliorates bisphenol A-induced colon damage: Inhibition of NADPH oxidase. *Journal of Agricultural and Food Chemistry*, 71, 2566–2578.
- Ye, X. L., Liu, Y., Hu, J. J., Gao, Y. Y., Ma, Y. A., & Wen, D. L. (2021). Chlorogenic acid-induced gut microbiota improves metabolic endotoxemia. *Frontiers in Endocrinology*, 12, Article 762691.
- Yue, Y. X., Wang, Y. Q., Xie, Q. G., Lv, X. L., Zhou, L. Y., Smith, E. E., & Ma, W. W. (2023). *Bifidobacterium bifidum* E3 Combined with *Bifidobacterium longum* subsp. *infantis* E4 improves Ips-induced intestinal injury by inhibiting the TLR4/NF- $\kappa$ B and MAPK signaling pathways in vivo. *Journal of Agricultural and Food Chemistry*, 71, 8915–8930.
- Zhang, H. L., Tian, S. S., Zhao, Q. L., Xu, Y. Z., Bi, L. J., Jiang, S., & Tang, Y. P. (2023). Non-targeted metabolomics reveals a modulatory effect of DHA-enriched phosphatidylserine in high fat-diet induced non-alcoholic fatty liver disease in mice. *Process Biochemistry*, 135, 22–32.
- Zhang, L. Y., Shi, H. H., Wang, C. C., Wang, Y. M., Wei, Z. H., Xue, C. H., Mao, X. Z., & Zhang, T. T. (2022). Targeted lipidomics reveal the effects of different phospholipids on the phospholipid profiles of hepatic mitochondria and endoplasmic reticulum in high-fat/high-fructose-diet-induced nonalcoholic fatty liver disease mice. *Journal of Agricultural and Food Chemistry*, 70, 3529–3540.
- Zhang, T. T., Xu, J., Wang, Y. M., & Xue, C. H. (2019). Health benefits of dietary marine DHA/EPA-enriched glycerophospholipids. *Progress in Lipid Research*, 75, Article 100997.
- Zhang, Y. L., Xu, Y. N., Zhang, L., Chen, Y. J., Wu, T., Liu, R., & Zhang, M. (2022). Licorice extract ameliorates hyperglycemia through reshaping gut microbiota structure and inhibiting TLR4/NF- $\kappa$ B signaling pathway in type 2 diabetic mice. *Food Research International*, 153, Article 110945.
- Zhao, H. J., Li, M., Liu, L., Li, D., Zhao, L. J., Wu, Z., & Yang, F. (2023). *Cordyceps militaris* polysaccharide alleviates diabetic symptoms by regulating gut microbiota against TLR4/NF- $\kappa$ B pathway. *International Journal of Biological Macromolecules*, 230, Article 123241.
- Zheng, S. L., Wang, Y. Z., Zhao, Y. Q., Zhu, W. Y., Chi, C. F., & Wang, B. (2023). High Fischer ratio oligopeptides from hard-shelled mussel: Preparation and hepatoprotective effect against acetaminophen-induced liver injury in mice. *Food Bioscience*, 53, Article 102638.
- Zhou, Y. F., Tian, S. S., Qian, L., Jiang, S., Tang, Y. P., & Han, T. (2021). DHA-enriched phosphatidylserine ameliorates non-alcoholic fatty liver disease and intestinal dysbacteriosis in mice induced by a high-fat diet. *Food & Function*, 12, 4021–4033.